Original Article

ISSN: 2788-8517 (online)
2788-9963 (Print)

Journal of Urban Development Studies
Vol. 3, Issue 2 (2023)

IMPLICATIONS OF URBAN LAND USE LAND COVER CHANGE ON LAND SURFACE TEMPERATURE AND THERMAL COMFORT: THE CASE OF ADDIS ABABA, ETHIOPIA.

Gebru Z. Abraha[a]* & Bisrat K. Arsiso[b]

[a]Department of Environment and Climate Change Management, Ethiopian Civil Service University. gebruze1990@gmail.com

[b]Assistant Professor at the College of Urban Development and Engineering in Ethiopian Civil service University. bisrat_k2002@yahoo.com

Received: 28 September 2023, revised: 15 November 2023, accepted: 21 November 2023

Abstract

Environmental domains such as surface temperature and accompanying thermal stress were most affected and will continue to be affected by the replacement of natural terrains with impervious surfaces (urban growth). GIS and remote sensing techniques are now receiving a lot of interest in detecting and analyzing such domains. This study examined the thermal comfort of the city using multispectral satellite images taken between 1991 and 2022. To analyze and display data in this study, applications such as ArcGIS 10.7, ERDAS IMAGINE2013, and Excel 2013 were used. Between 1991 and 2022, vegetation cover, agricultural land, and bare land lost a net of 54%, 28%, and 31%, respectively, while built-up land gained a net of 113%. Over the previous three decades, while the city's mean annual surface temperature has risen by 0.27°C. Furthermore, whereas land surface temperature and built-up areas are positively related, vegetation in the city is negatively related to land surface temperature. In 1991, 305.5 km^2 (57%) and 233.67 km^2 (43% of the study area fell into the excellent and worst ecological categories, respectively, while in 2022, approximately 244.46 km^2 (43%) and 294.7 km^2 (55%) of the city area's geographical coverage fall into the excellent and worst thermal condition categories, respectively. Overall, the city's thermal stress has grown during the last three decades. Appropriate techniques are necessary to boost the city's vegetation cover.

Keywords: Landsat image, ecological category, thermal stress, land use.

1. Introduction

Since the dawn of civilization, humans have altered the face of the Earth by gathering essential resources such as food, fiber, and freshwater. Between 1990 and 2015, the world forest lost approximately 129 million hectares (FAO, 2015), which is roughly the size of South Africa's landmass. Changes in the LULC are a vital expression of human interactions with the environment (Sharma, 2018), and they are characterized and influenced by a variety of factors in space and time at varying magnitudes (Suliman et al., 2020). The impact of urbanization on climate conditions, particularly thermal (LST) trends, is significant. LST has become the most serious concern in the last 50 years as a result of uncontrolled urbanization and rising energy demand (Hasnat et al., 2019).

High population growth, urbanization, and industrialization can all have a significant impact on LULC patterns (Adegbola et al. 2021), and convert the landscape to more impervious urban surfaces, all of which have significant effects on the natural environment and climate (Bisrat, 2017). Addis Ababa has experienced massive urbanization in terms of population growth (the decadal growth rate was 20.96 % between 2001 and 2011) and major changes in the LULC (built-up area increased from 25.7 % in 1985 to 59.64 % in 2015, while vegetation cover decreased from 16.6 % to 9.54 % between 1985 and 2015). (Samson, 2016). As a result, such increasing change can cause and pose a threat to the city's microclimate. According to Bisrat (2017), observed surface improvements such as infrastructure (roads, railways, buildings, and others) and city population growth have modified and will continue to modify the case study's microclimate.

Despite research on Addis Abeba's thermal comfort, such as Moisa et al. (2022) and Moisa and Gemeda (2022). Most of them placed less focus on how their outcomes were impacted by the atmospheric band noise. Additionally, they employed Landsat 7, which had a striking scene and has noise effect on the thermal result. The aim of the study is to analyze how urban LULCC has affected LST and thermal variance in Addis Ababa City from 1991 to 2022 using radiometrically corrected and enhanced remotely sensed satellite images in order to give urban planners, managers of the environment and climate, and creators of inclusive planning current and updated information. This has the potential to have a significant impact on natural resource management and the sustainable development of the city.

2. Materials and Methods

2.1. Study area

Geographically, the study area is located between 9° 1′ 48″ to 8° 8′ 32″ N Latitude and 38° 44′ 24″ to 38° 9′ 05″ E Longitude. The city is situated in the central highlands of the country and covers an area of approximately 526 km2, with a population of over 5 million at a growth rate of 4.42% (World Population Review, 2021). By Köppen-Geiger classification, the climate of the study area is categorized or dominated by the Cwb climate. In other words, Addis Ababa has a humid subtropical mild summer climate that is mild with dry winters, mild rainy summers, and moderate seasonality. According to the National Metrological Agency (NMA.2022), from the year 1991 to 2020 the maximum and minimum monthly temperature of the study area ranges between 31^{o}C to 25.4^{o}C and 14.1^{o}C to 10.3^{o}C respectively, whereas the range of mean monthly temperature was between 22.3^{o}C to 19^{o}C. The hottest and coldest months are May and December which had an average temperature of 20^{0}C and 16.5^{0}C respectively. On average, rainfall was very high in June, July, August, and September since these are rainy months, whereas January, February, March, April, October, November, and December are recorded low rainfall and are considered dry months.

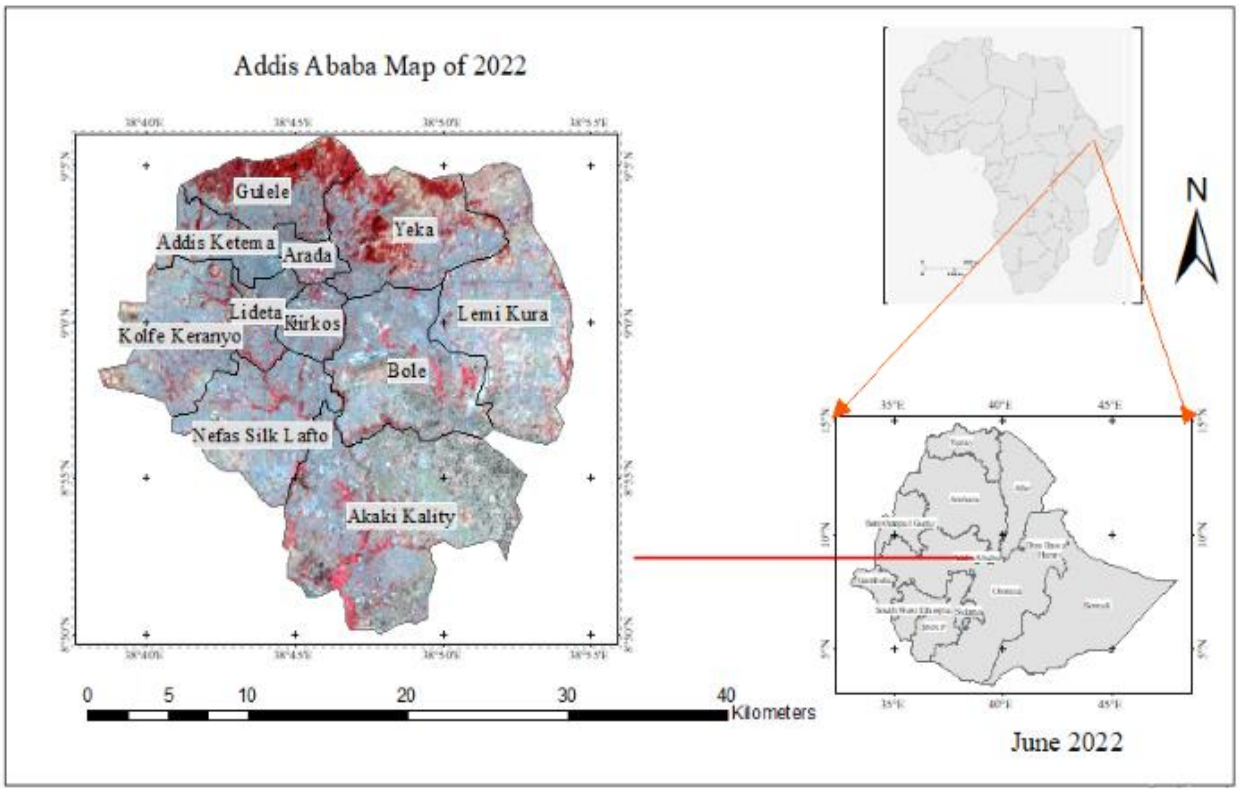

Figure 1. Location and administrative map

The study's main data were used satellite images (Landsat5, 8 and MODIS A12 data) which are downloaded from the United States Geological Survey (USGS) Earth Resources Observation System. The thermal bands of Landsat5 (band 6) and Landsat 8 (band 10) had 120m and 100m spatial resolution respectively and were resampled to 30m resolution in order to have the same resolution as those of Addis Ababa.

2.2. Data Description

band sets used for LULC classification. They are freely available at (https://earthexplorer.usgs.gov/).This study's datasets can be found at path code 168 and row code 054. Satellite images of Addis Ababa's sensed at a time of dry season months (March, April, and May), which are mostly cloud-free (WetherSpark, 2021) were selected for this study.

Satellite Data	Sensor	Date of Acquisition	Path/Row	Cloud Coverage
Landsat 5	TM	09/04/1991	160/054	0
Landsat 5	TM	23/03/2001	160/054	0
Landsat 5	TM	23/03/2011	160/054	0
Landsat 8	OLI/TIRS	26/03/2022	160/054	0

Table 1. Shows the Satellite imageries and Specifications used in this study

2.3. Method

The methodology used in this study is to utilize Geographic Information System and integration of the same with satellite imagery so as to yield good results in classification and quantification of LULCC, LST, and thermal stress for the study area. The overall methodological flow of the study used was illustrated as in figure (2) below;

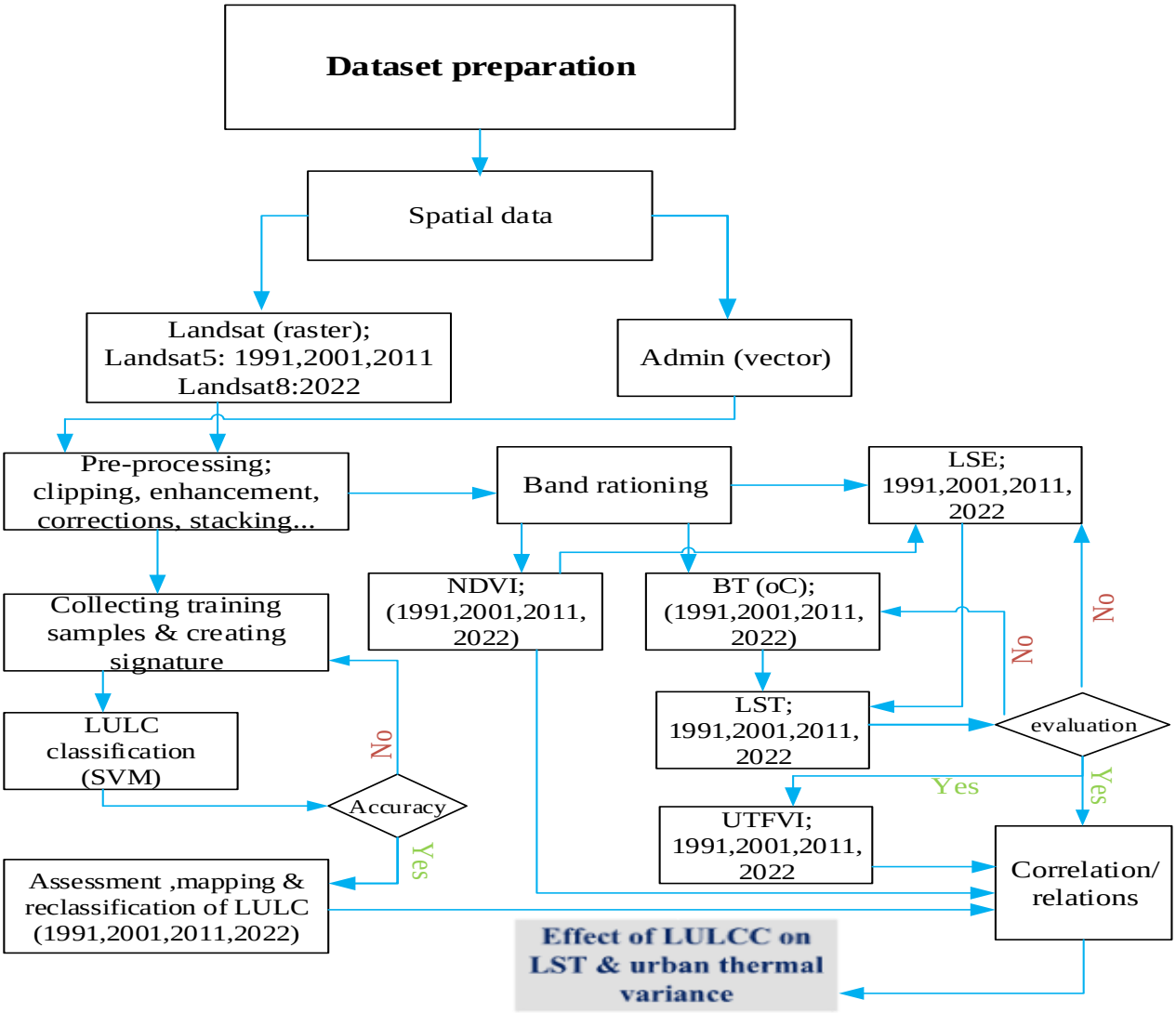

Figure 2. The methodological flow of the study.

3. Tools and Software

Before classifying and analyzing the collected data, two types of data correction preprocessing techniques was utilized in this study: (1) radiometric preprocessing, which addresses variations in pixel intensities (digital numbers, DN), and (2) geometric correction, which addresses errors in the relative positions of pixels, primarily due to sensor viewing geometry and terrain variations (Themistocles's and Hadjimitsis, 2008) using ERDAS IMAGINE and ENVI 5.3 software's.

3.1. LULC Analysis

To classify and extract various LULC types, the study used a supervised classification method. Thus, the researcher generated the spectral signatures of known categories, such as urban and forest, and the software allocates each pixel in the image to the cover type to which its signature is most comparable, according to (Eastman, 2003). To evaluate the accuracy of LULC classification result, Kappa coefficient, user accuracy and producer accuracy were calculated by confusion matrix method. This method was commonly used in similar studies (Wu and Murray, 2003; Thapa and Murayam, 2007). Lillesand et al. (2015) propose the following formula for assessing accuracy:

$$OA = \frac{Tp}{Tf} \dots\dots\dots\dots\dots Eq.(1)$$

Where;

OA = Overall accuracy

Tp = Total number of correctly classified pixels

Tf =Total number of reference pixels

$$UA = \frac{CCP}{TCP} \dots\dots\dots\dots Eq.(2)$$

Where;

UA= User Accuracy

CCP= Correctly Classified Pixels each class

TCP= Total Classified Pixels in that class

$$PA = \frac{CCP}{TCP} * 100 \dots\dots\dots Eq.(3)$$

Where;

PA= Producer Accuracy

$$K= \frac{N\left(\sum_{i=1}^{r} xii\right)-\left(\sum_{i=1}^{r}(xi+.x+i)\right)}{N^2-\sum_{i=1}^{r}(xi+.x+i)} \dots Eq.(4)$$

Where;

K= Kappa Coefficient

r = number of rows in the error matrix

Xii = number of observations in row i and column I (on major diagonal)

Xi+ = total of observations in row i (shown as marginal total to right of the matrix)

X+I = total of observation in column i (shown as margin total at bottom of the matrix)

N= total number of observations included in the matrix

3.2. Vegetation abundance analysis

Landsat Normalized Difference Vegetation Index (NDVI) is used to quantify vegetation greenness and is useful in understanding vegetation density and assessing changes in plant health (USGS, 2016). The values range from very low (<= -1) correspond to barren areas of rock, sand, or urban/built-up to very high (+1) indicate forest.

NDVI was calculated as (Abel, 2018, Bisrat, 2017, and Skokovic et al., 2014) Eq. (5):

$$NDVI = \frac{(NIR - Red)}{(NIR + Red)} \dots\dots\dots Eq.(5)$$

Where;

NDVI = Normalized Difference Vegetation Index

NIR = Reflectance in Near-infrared band

Red= Reflectance in the red band

Due to band composition differences between different Landsat types, there is differences in band reflectance measurements and NDVI was calculated differently as below:

In Landsat 4-7, NDVI = (Band 4 – Band 3) / (Band 4 + Band 3).

In Landsat 8, NDVI = (Band 5 – Band 4) / (Band 5 + Band 4).

3.3. Land Surface Temperature Analysis

To estimate terrestrial surface temperatures, radiometrically corrected thermal infrared bands of Landsat images, namely Landsat TM and ETM+ band 6 (thermal infrared band) and Landsat 8 Band 10 (thermal infrared band), were used to convert Digital Numbers (DNs) into radiance. The LST of the study, according to Avdan and Jovanovska (2016), was calculated as (Eq.6):

$$LST = \frac{BT}{\left\{1 + \left[\left(\frac{\lambda BT}{\rho}\right) \ln \varepsilon\lambda\right]\right\}} \dots . \text{Eq. (6)}$$

Where;

LST = Land Surface Temperature in Celsius (^oC)

BT = satellite temperature (at sensor) (^oC)

λ = the wavelength of emitted (11.5μm),

ρ = Constant value obtained by the formula $\rho = h * (c/\alpha) = 1.438 * 102$ mk (h = Planck's constant (6.626 * 1034 JS), c = velocity of light (2.998 * 108m/s) and α = Boltzmann constant (1.38 * 1023J/k)

$\varepsilon\lambda$ = surface emissivity using… Eq. (11)

3.4. DN Conversion to Radiance

The study used formula sated by USGS,2019 to convert Landsat 5 and 7 image pixels from DN to absolute radiance units as Eq (7):

$$L\lambda = \left(\frac{LMAX\lambda - LMIN\lambda}{QCALMAX - QCALMIN}\right) * (QCAL - QCALMIN) + LMIN\lambda \dots \text{Eq. (7)}$$

Where;

Lλ= TOA spectral radiance (Watts/(m2*srad *μm))

LMAXλ = Spectral radiance scaled to QCALMAX (found in metadata);

LMINλ = Spectral Radiance scaled to QCALMIN (found in metadata);

QCALMAX = Maximum quantized calibrated pixel value (corresponding to LMAXλ) in DN

QCALMIN = Minimum quantized calibrated pixel value (corresponding to LMINλ) in DN

QCAL = Quantized calibrated pixel value in DN

The formula given by USGS (2016) in the Landsat-8 data user handbook is used to convert the image pixels of Landsat 8 from DN to units of absolute radiance as Eq.(8).

$$L\lambda = (ML * Qcal) + AL \ldots\ldots \text{Eq. (8)}$$

Where:

Lλ= TOA spectral radiance (Watts/(m2*srad *μm))

ML= Band specific multiplicative rescaling factor from the metadata (RADIANCE_MULTI_BAND_x, where x is the band number)

AL= Band specific additive rescaling factor from the metadata (RADIANCE_ADD_BAND_x, where x is the band number)

Qcal= Quantized and calibrated standard product pixel values (DN)

3.5. Radiance to Temperature Conversion

According to a USGS handbook document published in 2019, radiance to brightness temperature conversions were made using the Planck equation as (Eq.9), and the given equation is subtracted by 273.15 to convert temperature from kelvin to Celsius.

$$T = \left(\frac{K2}{LN\left(\left(\frac{k1}{L\lambda}\right) + 1\right)} \right) - 273.15. \text{Eq. (9)}$$

Where;

T= Brightness temperature in Celsius

K2 and K1= calibration constant obtained from the metadata file

3.6. Land Surface Emissivity (LSE)

Surface emissivity stands for the ability of the surface to transform heat energy into radiant energy (Sobrino et al., 2001). Land surface emissivity (LSE) is the average emissivity of an element on the surface of the Earth and is calculated from the vegetation degree of coverage or vegetation proportion values calculated as (Eq.10) (Skokovic et al., 2014).

$$PV = [(NDVI - NDVI\ min))/(NDVImax - NDVImin)]2 \ldots. \text{Eq. (10)}$$

Where;

PV = proportion of vegetation

NDVI = DN values from Normalized Difference Vegetation Index image

NDVImin = minimum DN values from Normalized Difference Vegetation Index image

NDVImax = Maximum DN values from Normalized Difference Vegetation Index image

Then the value of the emissivity is obtained through (Eq.11):

$$e = m * PV + n \ldots\ldots \text{Eq. (11)}$$

Where;

e = surface emissivity

m = value of emissivity of vegetation, in this case 0.004 was used

PV = proportion of vegetation

n = Soil emissivity value, in this case 0.986 was used

Finally, surface emissivity is calculated as (Eq.12)

$$e = 0.004 * PV + 0.986 \ldots\ldots \text{Eq. (12)}$$

Where;

e = land surface emissivity

PV = proportion of vegetation

3.7. LST Result Evaluation

The extracted result of the LST of the study area in the year 2022 was evaluated using

MODIS 11 A2 of the year 2022 data.

The MODIS land surface temperature and emissivity products at 1 km spatial resolution and 8-day temporal resolution are retrieved in the Hierarchical Data Format (HDF-EOS) from the USGS Earth Explorer website. This HDF format was converted to an image format using ArcGIS software. Finally, the results of both sensors were compared.

3.8. Thermal Comfort Assessment through UTFVI

The study used UTFVI to analyze the thermal stress of the study area, which is the most widely used statistic for evaluating urban environments from an ecological perspective (Naim and Kafy, 2021; Abir et al., 2021; Al Faisal et al., 2021).

The UTFVI was computed (S. Ahmed, 2018) as Eq. (13):

$$\text{UTFVI} = \frac{\text{TS} - \text{Tm}}{\text{Tm}} \dots\dots \text{Eq. (13)}$$

Where;

UTFVI = Urban Thermal Field Variance Index

TS = Land Surface Temperature (LST)

Tm = the mean LST of the area.

Urban Thermal Field Variation Index (UTFVI)	Status of thermal comfort
< 0	Excellent
0 - 0.005	Good
0.005 - 0.010	Normal
0.010 – 0.015	Bad
0.015 – 0.020	Worse
> 0.020	Worst

Table 2. Threshold UTFVI value for ecological evaluation and thermal comfort. Abir et al 2021

3.9. Statistical Analysis

3.10.

In this study, the LULC was assessed quantitatively using a transmission matrix. The correlation function was also used to establish quantifiable relationships of NDVI and NDBI, with the LST in the study area, which is implemented using the ArcGIS and Excel 2016 software packages.

4. Results and Discussion

4.1. Spatial Analysis of LULCC

During the year 1991, the southeastern part of the city was dominated by bare land and agriculture classes, while vegetation cover dominated the northern, north-eastern, and northwestern parts of the city. The built-up area was mostly concentrated in the central part of the city. From the year of 1991 to 2011, the agricultural land class expanded, especially in the southeastern part of Addis Ababa (Figure 3A to 3C). However, after the year of 2011, it started to decline sharply (Figure 3, D). Overall, the result shows the expansion of built-up areas at the expense of the other three land classes (agriculture, bare land, and vegetation). This is due to the need for more land for developmental activities.

As shown in Figure (4b), except for some parts of Gulele and Yeka, and the riverside areas; vegetation cover gradually diminished or sharply declined from the year 1991 to 2022, as a result of the built-up cover expansion. Similarly, in the year 2022 except for the Northern and North-eastern parts of Akaki Kality, some parts of South-eastern Bole, the Southern part of Lemi Kura, and the riverside parts of the city; agricultural land is shrinking (Figure 4b). On the contrary, except for Arada, Lideta, and Kirkos sub cities which are previously covered by built-up and still are (Figure 4a), the built-up class was sharply increasing almost around all other sub-cities expense of the vegetation and bare land classes of the city

.

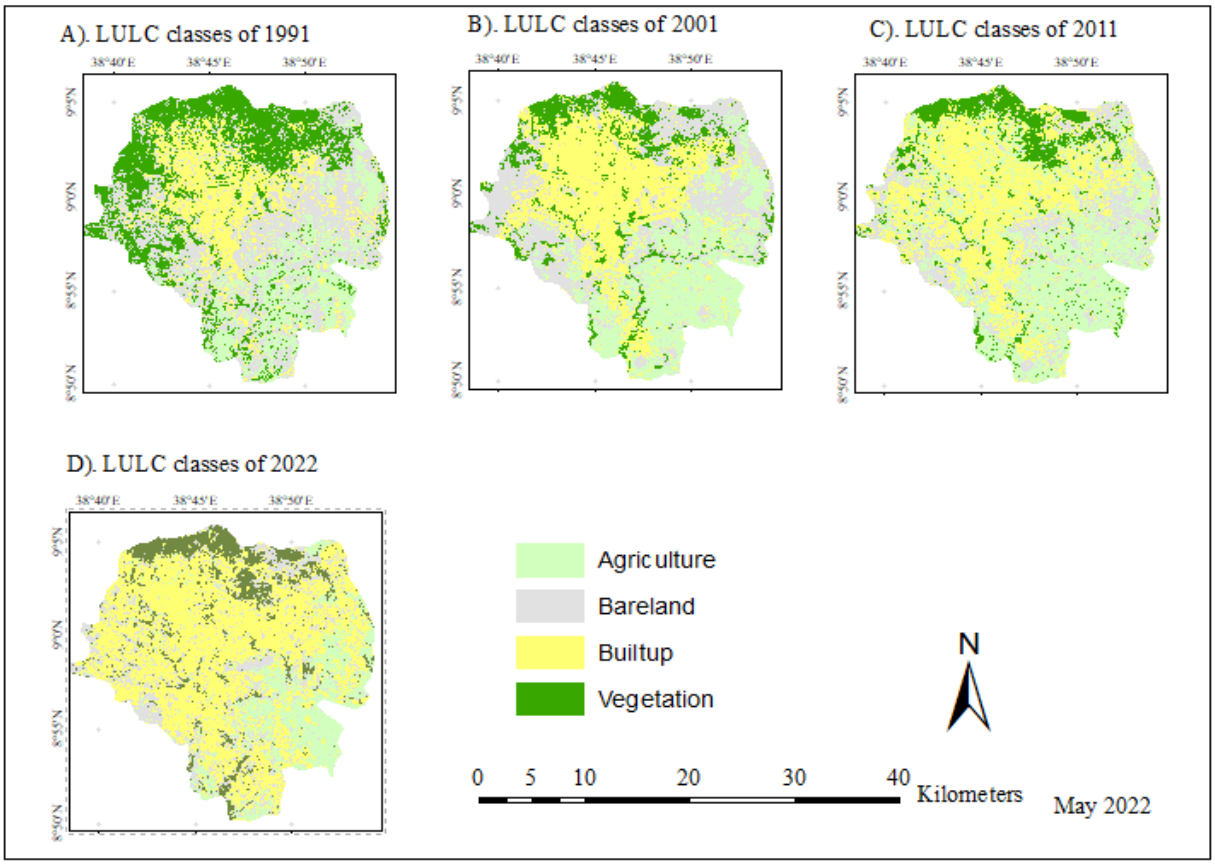

Figure 3. LULC map of Addis Ababa (between 1991 to 2022)

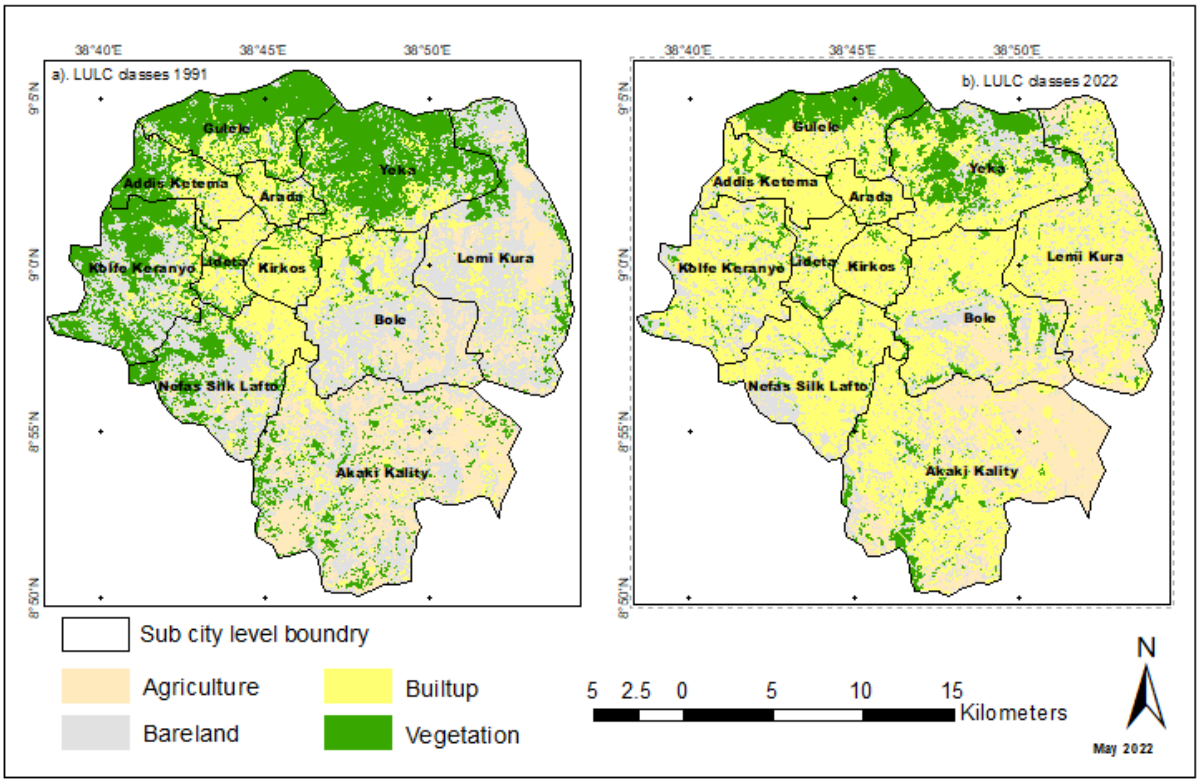

Figure 4. LULC map sub-city level (1991 and 2022).

4.2. LULC Area Statistical Analysis Approximately 27%, 13%, 12%, and

12 % of the study area was covered by vegetation in 1991, 2001, 2011, and 2022, respectively (Table 4). During the same time period, the built-up area accounted for 22%, 33%, 35%, and 53%, respectively. The coverage of agricultural areas in 1991, 2001, 2011, and 2022 was about 16%, 25%, 34%, and 16% of the total area under study, respectively; and approximately 34%, 29%, 19%, and 18% of the city's geographic area were classified as bare land, respectively of time of years.

In the year 1991, bare land covered approximately 188.1 km^2, which is 34% of the total geographical area of the city. In the year 2022, it dropped by almost more than half, approaching 97.56km^2. On the other hand, approximately 10 km^2 of other than built-up features classes were converted to built-up land annually in the last three decades (Table 4).

Between 1991 and 2022 vegetation land class has been lost 66% and gained 12% having a net loss of 54%. However, the built-up area gained more, unlike the other land use land cover classes. Thus, built-up land has been lost 23% and gained 136% with a net gain of 113% (Table 5). Generally, from 1991 to 2022, an average of 5.8 km^2 of land was converted to development in Addis Ababa per year. This was merely due to the rising demand for land for different developmental purposes.

LULC classes	1991		2001		2011		2022	
	Area(km²)	%	Area(km²)	%	Area(km²)	%	Area(km²)	%
Bu	122.92	22%	177.12	33%	211.51	39%	286.61	53%
Vg	147.86	27%	71.76	13%	63.79	12%	66.9	12%
Ag	90.26	16%	135.65	25%	145.31	27%	88.06	16%
B1	188.1	34%	154.59	29%	118.53	22%	97.56	18%
Total	549.14	100%	539.12	100%	539.14	100%	539.13	100%

Table 3. Show the quantitative area coverage of each LULC class in Addis Ababa (1991 to 2022).

	LULC classes	LULC classes 2022									
		Ag		Bl		Bu		Vg		Total	
		km²	%	km²	%	km²	%	km²	%	km²	%
LULC classes 1991	Ag	36.39	40%	13.31	15%	38.07	42%	2.46	3%	90.23	100%
	Bl	31.84	17%	40.6	22%	103.9	55%	11.7	6%	188	100%
	Bu	9.42	8%	13.61	12%	86.64	77%	3.23	3%	112.9	100%
	Vg	10.33	7%	29.98	20%	57.94	39%	49.5	34%	147.8	100%
	Total	87.98	16%	97.5	18%	286.6	53%	66.9	12%	538.9	100%

Where: Bu=Built-up, Vg=Vegetation, Ag= Agriculture, and Bl= Bare land

Table 4. Show the LULC class's coverage change matrix (1991 to 2022)

4.3. Accuracy Assessment

The accuracy assessment results in Table (5) show that the overall accuracy obtained from the random sampling process for 2022 is approximately 92.8%. The range of user accuracy ranges from 90.4% to 99%, which shows the reliability of the classification in the study. Vegetation, on the other hand, was found to be relatively more reliable, with 99 % user accuracy. The overall Kappa

coefficient was approximately 0.90, which is recognized excellent classification.

	Class types determined from reference sources						User Accuracy
	Land classes	Ag	Bl	Bu	Vg	Total	
Class types determined from classified map	Ag	85	0	1	0	86	98.84%
	Bl	5	94	5	0	104	90.40%
	Bu	3	9	227	1	240	94.60%
	Vg	10	4	1	100	115	99%
	Total	103	107	234	101	545	
Producer Accuracy		82.50%	87.90%	97%	87%		Total=92.8%
Overall Accuracy	92.80%						
Kappa Statistic	89.80%						

Table 5. Shows the accuracy assessment error matrix (2022)

4.4. Vegetation Abundance Analysis through NDVI

Due to the horizontal expansion of built-up areas, the areas covered by vegetation (higher NDVI values) have shrunk dramatically over the last three decades in the city. As a result, in 2022, areas with high NDVI values were shrinking and only available around the Menagesha, Entoto, Yeka Michael, and riverside areas of the city (NDVI value of 0.59).

Despite advocacy and programs for tree planting as part of the national green economy strategy, the maximum NDVI value has decreased in the three decadal years of 1991, 2001, and 2022, representing 0.85, 0.64, 0.68, and 0.59, respectively (Table 6). According to the findings of this study, the spatial extent of vegetation cover was much greater in 1991 than in 2022. This is due to the expansion of local surface impervious or urban development at the expense of vegetation, which has an impact on the surrounding vegetation types and has effect on the local climates of the city. This reveals that not only shrinking in size but also vegetation health is thriving and relatively under stress in the city. And also tells, there is a decrease in the productivity of the forest and or decreasing solar absorption capacity and exposing the land to solar radiation.

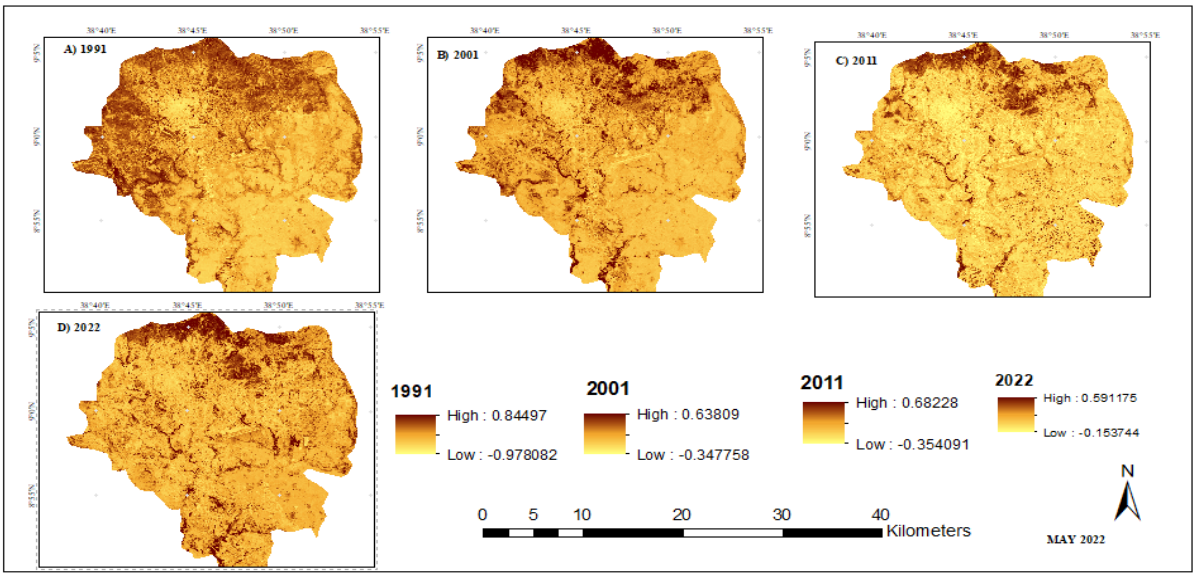

Figure 5. Shows the spatio-temporal pattern of NDVI in Addis Ababa (1991 to 2022)

NDVI	1991	2001	2011	2022
MIN	-0.98	-0.35	-0.36	-0.16
MAX	0.85	0.64	0.68	0.59
MEAN	0.25	0.01	0.05	0.13
STD	0.15	0.1	0.14	0.07

Where: MIN = Minimum, MAX = Maximum, STD = Standard deviation

Table 6. Shows the statistical pattern of NDVI in Addis Ababa (1991 to 2022)

4.5. Analysis of Distribution of LST
4.6. and its Responses to LULC types

The city's LST pattern had shifted dramatically within the three decades. For instance, except for the northern part of the city which is stretching from Gulelle to Yeka Mickael and the riverine area, most parts of the city had high LST in 2022, which is associated with a transition of other natural terrains to build up land use (Figure 6). There is a variation in the value of LST in the built-up area as a consequence of the activities like industrial areas, densely settled areas, and developments on bare lands. For instance, of the eleven (11) sub-cities, Akaki Kality and some parts of the Bole sub-city recorded the highest LST compared to the other sub-cities (Figure 6). In the study area, the built-up and bare land areas are the land use categories that are significantly linked to great mean and maximum LST because of their land surface properties such as lack of shading from vegetation cover, more imperious surface, and dense buildings. The lowest mean land surface temperature corresponded to areas covered by vegetation. Statistically, the mean LST of the city in the year of 1991, 2001, 2011, and 2022 registers 24.25^{o}C, 29.89^{o}C, 30.49^{o}C, and 32.34^{o}C respectively (Table 11). It is found that approximately 62% and 71% of areas of the city fell in the highest temperature zone (>30 °C) in 2001 and 2022, respectively. Moreover, the average LST increased from 24.25^{o}C to 32.34^{o}C from 1991 to 2022. The mean surface temperature of Addis Ababa increased by 8.09^{0}C during the three decades. This means that the mean annual surface temperature of

the city is increased by 0.27°C annually. According to the result, the expansion of built-up areas in the study area contributed directly and indirectly to the variation of the local urban climate. The direct impact is related to rising surface temperatures caused by the expansion of industries, housing projects, roads, transportation, and other human activities. Indirect effects are based on the effects of these activities on forest coverage, which reduces or eliminates the cooling effect. It is observed that in Addis Ababa the overall average annual temperature increased due to the process of urbanization which is mainly the expansion of built up

.

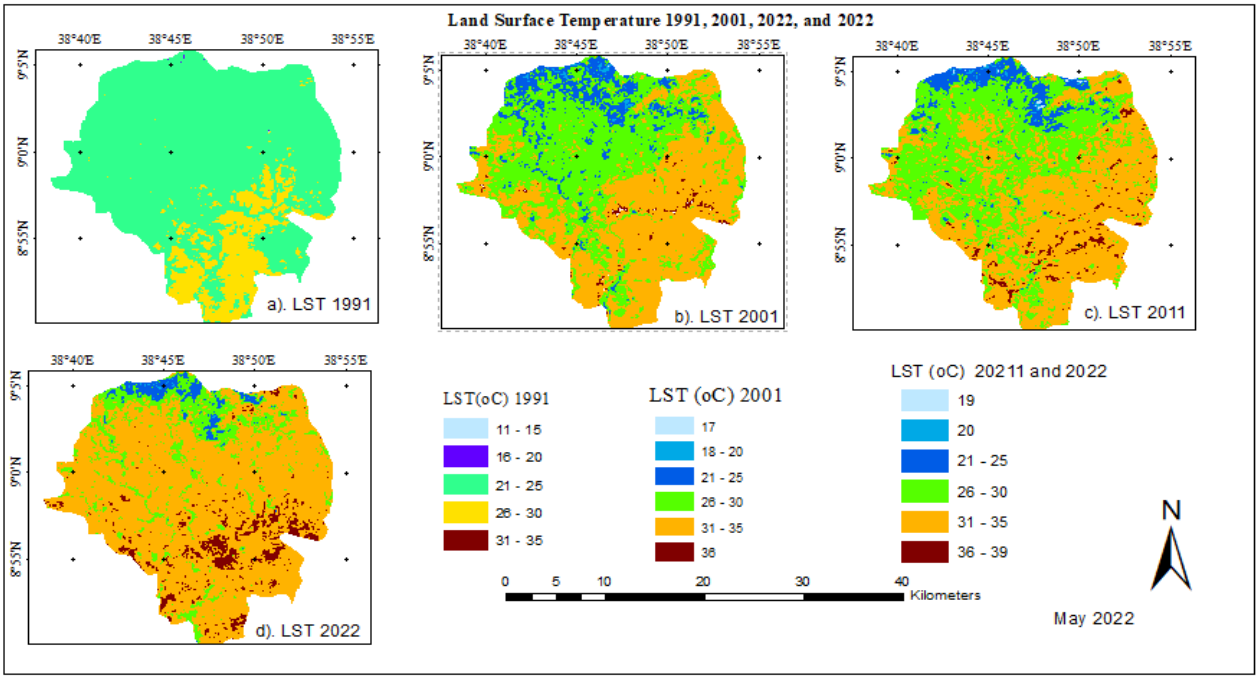

Figure 6. Shows the spatial and temporal variation of LST (°C) in Addis Ababa (1991 to 2022)

LST (°C)	1991	2001	2011	2022
MIN	11	17	17	18
MAX	35	38	40	40
MEAN	24.25	29.89	30.49	32.34
SD	1.3	3.21	3.19	2.69

Where: MIN = Minimum, MAX = Maximum, STD = Standard deviation

Table 7. Shows the temporal variance in LST (°C) ,1991 to 2022.

4.7. Relationship of LST with Vegetation and Built-up

The relationship between NDVI and LST in 2022 is expressed by the coefficient of determination (R^2) value of 0.9704 (Figure 16). This indicated that LST has a strong negative correlation with vegetation fraction. LST has a strong positive correlation with NDBI, which is having a coefficient of determination (R2) value of 0.962 (Figure 7). Thus, the built-up area was significantly linked to mean and maximum LST very likely because of its land surface properties such as lack of shading from vegetation cover, more imperious surface, dense buildings, and concrete surfaces (Figure 8). The mean LST of built-up and vegetation class in 2022 was 33.4°C and 28.3°C respectively. This shows that in the study area there is an experience of higher LST value or there is the reduction or elimination of the land

used for cooling effects such as the replacement of vegetation and water body by impervious s surfaces (built-up and bare land). The researcher argued that vegetation has a significant role in balancing local climates particularly to control the LST of the city. This is because the release of water vapor during photosynthesis and alters surface energy fluxes, which leads to potential cloud formation, which alters the amount of sunlight or radiation that can reach the Earth, affecting the Earth's energy balance (Evarts, 2017).

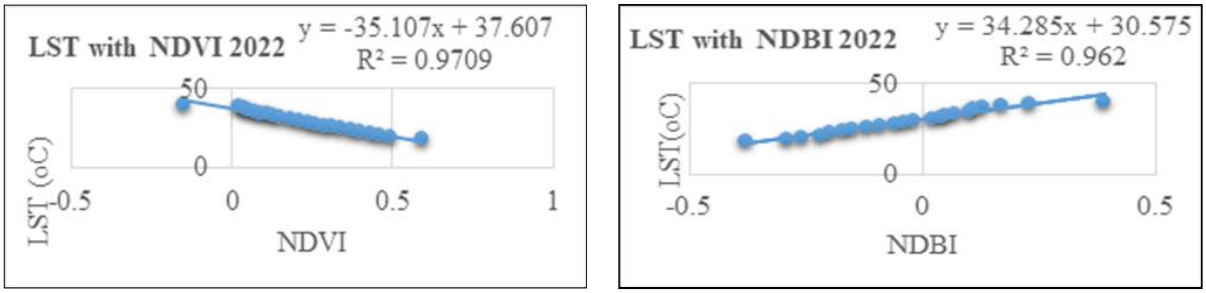

Figure 7. Correlation between LST and NDVI (in Addis Ababa (2022) (left) and Correlation between LST and NDBI in Addis Ababa (2022) (right).

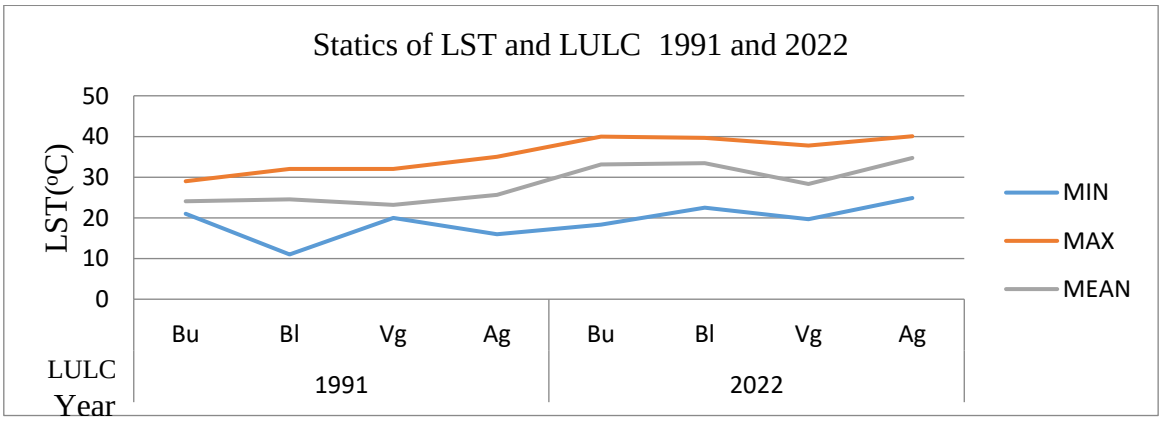

Figure 8. LST (°C) corresponds to different LULC classes in Addis Ababa (1991 and 2022).

4.8. Evaluation of LST by MODIS 11A2

Over the study area, the LST variances extracted from both thermal band sensors were close to each other. For instance, in 2022, the LST result extracted from the thermal band (band 10) of Landsat 8 ranges from 40°C to 18°C, while the coarse resolution MODIS 11 A2-based LST ranged from 38.91°C to 23.81°C (Figure 9). This indicates that the result of LST for this study was likely very confident.

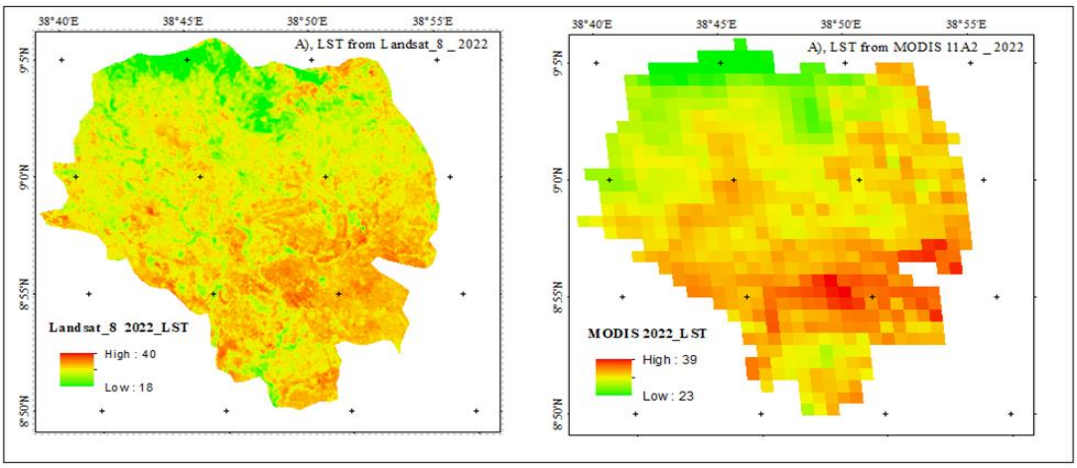

Figure 9. Evaluation of LST Landsat 8 (left) by MODIS-based LST (right) (2022)

4.9. Thermal Comfort Assessment through UTFVI

It is evident that the city experienced two extreme categories of eco-logical evaluation: excellent (UTFVI < 0) and poor (UTFVI > 0.020) (Table 8 and Figure 10). Spatially, the excellent thermal conditions are mostly found in northern, northwestern, north-eastern, and river-side areas of the city. However, the worst category (i.e., UTFVI > 0.020) exists around the central, southern, and southeastern parts of the study area. This is due to; the majority of the land is impervious in nature (either bare land with an exposed rock surface or built-up areas).

According to the findings, in 1991, 305.5 km^2 or 57% and 233.67 km^2 or 43% of the area of the city fell into the excellent and worst categories, respectively. The area under excellent thermal conditions has decreased over time and now accounts for 244.46 km^2, or 43% of the city's total area, in 2022. On the other hand, the area affected by the worst UTFVI phenomenon increased to 294.7 km^2 or 55% in 2022. Thus, the excellent ecological zones of the city have shrunk dramatically over the years, while the worst ecological zones have expanded significantly. The results of the seasonal UTFVI analysis highlight the city's gradual degradation of habitability. Thus, the researcher argued that, due to the expansion of individuals' interest-wise urbanization, there is an increase in discomfort in the thermal condition in the city.

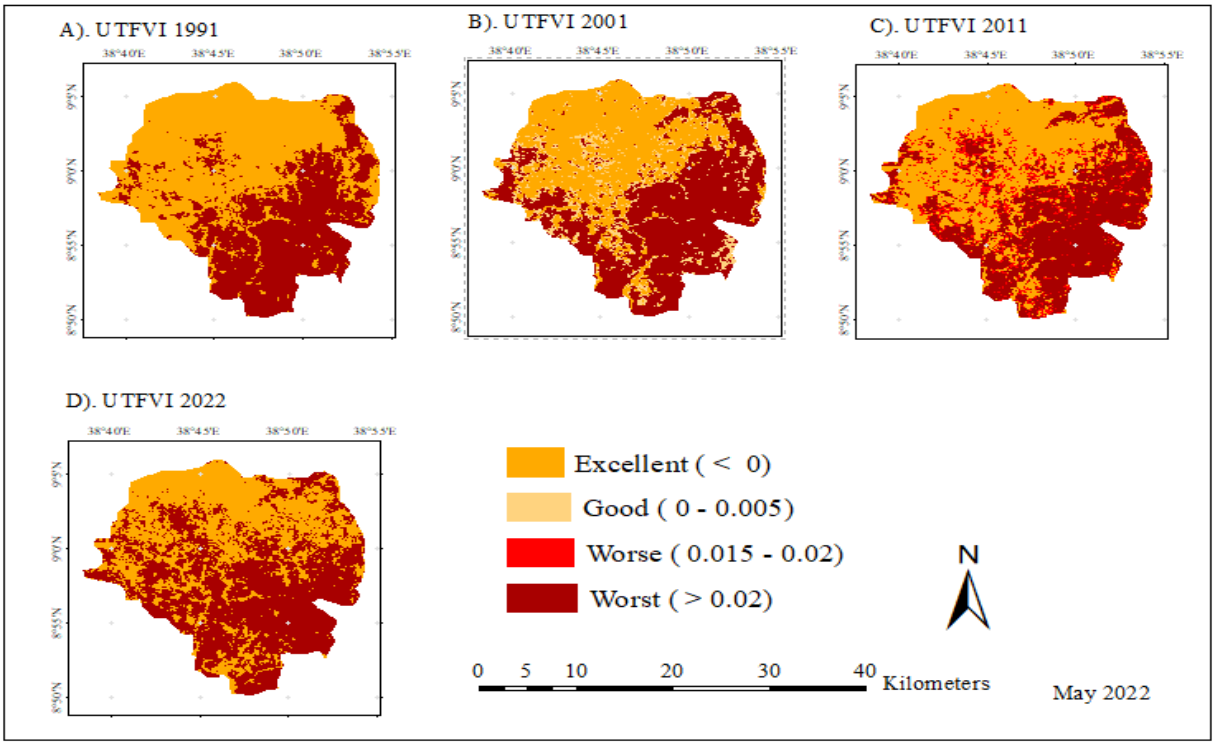

Figure 10. Shows the spatial distribution of thermal comfort in Addis Ababa (1991 to 2022)

	1991		2001		2011		2022	
EEI	Area (km²)	%	Area (km²)	%	Area (km²)	%	Area (km²)	%
Excel-lent	305.5	57%	214.92	40%	249.75	46%	244.46	45%
Good			65.83	12%				
Worse					63.62	12%		
Worst	233.67	43%	258.4	48%	225.8	42%	294.7	55%
Total	539.17	100 %	539.15	100 %	539.17	100 %	539.16	100 %

Where: EEI=Ecological Evaluation Index

Table 8. Distribution of thermal comfort areal coverage in Addis Ababa (1991 to 2022).

5. Conclusions

In the study area, the natural terrain was replaced by the impervious landscape. Unlike the other land use feature classes, urban built-up has grown significantly in the last three decades, at the expense of vegetation, agriculture, and bare lands. Approximately about 10 km^2 of city land has been converted to built-up land on an annual basis.

Also, with regard to LST, the mean surface temperature of Addis Ababa increased by

8.09ºC during the last three decades, i.e., from 24.25ºC in 1991 to 32.34ºC in 2022. This means that the mean annual surface temperature of the city is increased by 0.27ºC annually. Moreover, related to the response of LST to LULC classes, LST and built-up areas have a positive relationship, while LST has a negative correlation with vegetation in the study area.

In 1991, 305.5 km^2 or 57% and 233.67 km^2 or 43% of the geographical coverage of the city area were under the excellent and worst ecological category, respectively, while in 2022, about 244.46 km^2 or 43% and 294.7 km^2 or 55% fell under the excellent and worst thermal condition categories. This showed that in the past three decades, about 61 km^2 of the land area of the city was changed from an excellent ecological category to the worst category. Moreover, the city has experienced stressful thermal ecology in the southern and central parts. This is due to the replacement of vegetation with impervious surfaces mostly settlements exacerbated the thermal condition of the city.

The researcher believes this work can contribute to the urban environment sustainability field of study by opening ways for multidivisional decision-making and multidisciplinary planning approaches. Urban managers and administrations can initiate to take appropriate and sound decisions toward urban sustainable development.

Acknowledgment

The author would like to express his gratitude to the United States Geological Survey (USGS) Earth Explorer and Ethiopian National Meteorological Agency (NMA) for providing the Landsat archives.

References

Abir, F. A., Ahmmed, S., Sarker, S. H., & Fahim, A. U. (2021). Thermal and ecological assessment based on land surface temperature and quantifying multivariate controlling factors in Bogura, Bangladesh. Heliyon, 7(9), 1-12. https://doi.org/10.1016/j.heliyon.2021.e08012

Adegbola, P. A., Adewumi, J.R. & Okeke, O.O. (2021). Application of Markov Chain Model and ArcGIS in Land Use Projection of Ala River Catchment, Akure, Nigeria. Nigerian Journal of Technological Development, 18 (1). DOI: 10.4314/njtd.v18i1.5

Al-Faisal,A.,Al-Kafy,A.,Al Rakib,A.,Akter,K.S.,Jahir,A.D.,Sikdar,S.,…Rahman,M., (2021). Assessing and predicting land use/land cover, land surface temperature and urban thermal field variance index using Landsat imagery for Dhaka Metropolitan area. Environmental Challenges, 4(2021), 100192. https://doi.org/10.1016/j.envc.2021.100192

Avdan, U. & Jovanovska, G. (2016). Algorithm for Automated Mapping of Land Surface Temperature Using LANDSAT 8 Satellite Data. Hindawi Publishing Corporation. Journal of Sensors, Volume 2016, Article ID 1480307, 8. http://dx.doi.org/10.1155/2016/1480307

Bisrat, K.A., (2017). Trends in Climate and Urbanization and Their Impacts on Surface Water Supply in The City of Addis Ababa, Ethiopia. [Unpublished Doctor of Philosophy thesis]. University of South Africa.

Bisrat, K.A., Stoffberg, G.H., & Gizaw, M.T. (2018). Signature of present and projected climate change at an urban scale: The case of Addis Ababa. Physics and Chemistry of the Earth 105 (2018) 104–114.https://www.researchgate.net/publication/324007598

Eastman, J.R. (2003). Guide to GIS and Image Processing (Volume 1). Idrisi production. Clark University Manual, USA.

https://academic.uprm.edu/~jchinea/cursos/gis/lectesc/Kilimanjaro%20Manual.pdf

Evarts, H., (2017). How vegetation alters climate. Stanford Earth Matters; climate change.

Retrieved from https://earth.stanford.edu/news/how-vegetation-alters-climate#gs.zcae51

FAO. Global Forest Resources Assessment (2015). How are the World's Forests Changing? 2nd ed.; Food and Agriculture Organization of the United Nations: Rome, Italy, 2016.

Hasnat, G.N.T., Kabir, M.A., & Hossain, M.A., (2019). Major Environmental Issues and Problems of South Asia, Particularly Bangladesh, Handbook of Environmental Materials Management. https://doi.org/10.1007/978-3-319-73645-7_7

Lillesand, T. M., Kiefer, R. W., & Chipman, J. W. (2015). Remote Sensing and Image Interpretation. 7th ed. John Wiley & Sons, Inc. USA.

Moisa, M.B., Dejene, I.N., Roba, Z.R. et al (2022). Impact of urban land use and land cover change on urban heat island and urban thermal comfort level: a case study of Addis Ababa City, Ethiopia. Environ Monit Assess 194, 736 (2022). https://doi.org/10.1007/s10661-022-10414-z

Moisa, M.B. & Desalegn, G.O (2022). Assessment of urban thermal field variance index and thermal comfort level of Addis Ababa metropolitan city, Ethiopia. Haliyon 8, 8, E10185, 2022. DOI:https://doi.org/10.1016/j.heliyon.2022.e10185

Naim, M.N.H., & Kafy, A. A., (2021). Assessment of Urban Thermal Field Variance Index and defining the relationship between land cover and surface temperature in Chattogram city: a remote sensing and statistical approach. Environmental Challenges 100107. doi:10.1016/j.envc.2021.100107, https://doi.org/https://doi.org/

Samson, W.L., (2016). Assessing the Impacts of Urban Green Areas on Mitigating Urban Heat Island Effect: The Case of Addis Ababa, Ethiopia. [Unpublished master's thesis]. Addis Ababa University.

Sharma, R. (2018). Changing Consumption Patterns—Drivers and the Environmental Impact, Sustainability 10, no. 11: 4190. https://doi.org/10.3390/su10114190

Skokovic, D., Sobrino, J., Jimenez, J, Barres,G.S., Julien,Y.,Mattar,C.,& Rossello,J.C.,(2014). Calibration and validation of land surface temperature for Landsat 8-tirs sensor. LPVE (Land product validation and evolution). https://www.researchgate.net/figure/Comparison-between-Landsat-and-MODIS-surface-temperature_tbl1_260631636

Thapa, R.& Murayama, Y. (2007). Image classification techniques in mapping urban landscape: A case study of Tsukuba city using AVNIR-2 sensor data. Tsukuba Geoenviron Ment. Science. 2007, 3, 3–10.

Themistocleous, K. & Hadjimitsis, D., (2008). The importance of considering atmospheric correction in the pre-processing of satellite remote sensing data Intended for the management and detection of cultural sites: a case study of the cyprus area.

USGS, (2016). Landsat 8 Handbook. Retrieved from. Retrieved from https://www.usgs.gov/media/files/landsat-8-data-users-handbook.

World Population Review, (WPR). (2021). Addis Ababa Population 2021. Retrieved, from https://worldpopulationreview.com/world-cities/addis-ababa-population

Wu, C. & Murray, A.T (2003). Estimating impervious surface distribution by spectral mixture analysis. Remote Sensing and Environment 2003, 84, 493–5